

CERN-TH/95-282
FERMILAB-Pub/95-369-T

QCD CORRECTIONS TO W BOSON PLUS HEAVY QUARK PRODUCTION
AT THE TEVATRON

WALTER T. GIELE, STEPHANE KELLER

*Fermilab, MS 106
Batavia, IL 60510, USA*

and

ERIC LAENEN

*CERN TH-Division
1211-CH, Geneva 23, Switzerland*

Abstract

The next-to-leading order QCD corrections to the production of a W -boson in association with a jet containing a heavy quark are presented. The calculation is fully differential in the final state particle momenta and includes the mass of the heavy quark. We study for the case of the Tevatron the sensitivity of the cross section to the strange quark distribution function, the dependence of the cross section on the heavy quark mass, the transverse momentum distribution of the jet containing the heavy quark, and the momentum distribution of the heavy quark in the jet.

CERN-TH/95-282
FERMILAB-Pub/95-369-T
November 1995

1. Introduction

The study of jet production in association with a vector boson at hadron colliders has been successful in the recent past. The advantage of this signal over pure jet production is that the lepton(s) from the vector boson decay can be used as a trigger, such that jets can be studied free from jet-trigger bias. Furthermore, the lower rate obviates the need for prescaling. On the theory side, the recent progress in calculational techniques to construct next-to-leading order (NLO) Monte-Carlo programs [1] has allowed a meaningful confrontation with data [2].

The tagging of heavy hadrons in the jet offers a unique possibility of studying the hadronic structure inside the jet. By considering jets where the *leading* hadron is tagged, a clear connection can be made with perturbative QCD. At the parton level, the tagging of a heavy hadron corresponds to the tagging of a heavy-flavor quark. Experimentally, the presence of a D or B meson is inferred through its decay products (e.g. CDF has recently investigated $\gamma + D^{*\pm}$ meson production, where the $D^{*\pm}$ meson was fully reconstructed [3]). Heavy flavor tagging has become much more efficient with the advent of secondary vertex detectors [4] and its importance has been clearly demonstrated in the analysis that led to the top quark discovery [5]. In the future, heavy flavor tagging will continue to be an important analysis tool. It will provide more detailed information about the event, as well as a test of the underlying QCD theory. See, e.g., the recently outlined program to extract parton densities exclusively from collider data [6].

If one demands the presence of a *charm* quark in the jet recoiling against a W -boson, the signal is directly sensitive to the strange quark distribution function in the proton, at a scale of the order of the W -mass. A detailed investigation of this case has been performed in [7] with the shower Monte-Carlo program PYTHIA [8].

Replacing the charm quark by a *bottom* quark, one could use this process as an alternative calibration of the b -quark tagging efficiency. This will be useful at luminosities achieved by the Main Injector. However, by far the dominant contribution to W +bottom production is due to $W + b\bar{b}$ production, where the heavy quark pair is produced by gluon splitting. Here the inclusion of the gluon to B meson fragmentation function is probably more important than the inclusion of NLO effects to the W +bottom process. This in turn would imply that this reaction could be used to constrain this fragmentation function.

We present here the calculation of the QCD corrections up to $O(\alpha_s^2)$ of the process $p\bar{p} \rightarrow W + Q$ where Q is an heavy quark. We keep the mass of the heavy quark explicit. In this letter we study the basic aspects of this process. Full details of the calculation method and more extensive phenomenological studies will be published separately [9].

This letter is organized as follows. In section 2, the method used to calculate the QCD radiative corrections is briefly outlined and some consequences of their inclusion are examined. The impact of the higher order corrections on the measurement of the strange quark distribution is discussed in section 3. In section 4, we study several aspects of the behavior of the heavy quark tagged jets. Finally, in section 5 our conclusions are presented.

2. Method

In this section the method used to calculate the $O(\alpha_s^2)$ QCD corrections to $p\bar{p} \rightarrow W + Q$ is outlined. It consists of a generalization of the phase space slicing method of Ref. [10] to include massive quarks. One of the strengths of this method is that it allows for the implementation of experimental cuts without the analytic recalculation of phase space integrals.

The leading order (LO) calculation is very simple and involves the two Feynman diagrams given in Fig. 1.

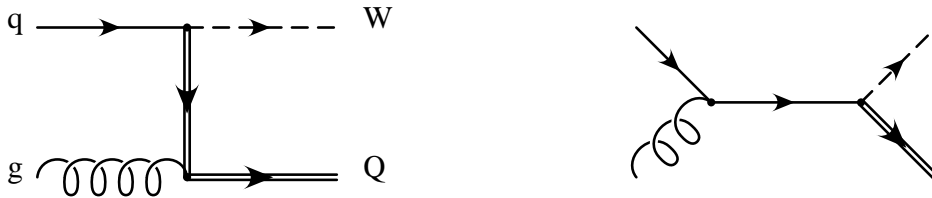


Figure 1: *The Born graphs for $W + Q$ production in $p\bar{p}$ collisions.*

The virtual corrections consist of the interference between the lowest order diagrams and their one-loop corrections. In order to regularize the various singularities in the integrals over the loop momenta we performed the integration in $d = 4 - 2\epsilon$ dimensions. The d -dimensional version [11] of the Passarino-Veltman reduction formalism [12] was used to reduce tensor and vector integrals to scalar ones. We made use of the algebraic manipulation program FORM [13] for much of the algebra. Some of the scalar integrals were not yet available in the literature, they will be listed in Ref. [9]. The ultraviolet singularities were absorbed through mass and coupling-constant renormalization. For the former we used the on-shell scheme and for the latter the $\overline{\text{MS}}$ scheme modified such that the heavy quarks decouple in the limit that small momenta flow into the heavy quark loops [14]. The remaining soft and collinear singularities, appearing as $1/\epsilon^2$ and $1/\epsilon$ poles, factorize into a universal factor multiplying the Born cross section.

The real corrections consist of the contributions from all the subprocesses $ij \rightarrow WQk$, where i, j, k are massless partons, and the subprocess $ij \rightarrow WQ\bar{Q}$ [15]. Some of these contributions exhibit soft and/or collinear singularities. In this paper we treat the heavy quark as extrinsic to the nucleon, hence we do not consider diagrams where the heavy quark is in the initial state. The method we used to isolate the singularities consists of slicing up the phase space and dividing it into a hard region, containing no singularities, and a region in which the final state parton is either soft or emitted collinearly with one of the initial state partons. Note that when a gluon is radiated from the heavy quark, the collinear singularity is shielded by the presence of the heavy quark mass. The hard region is defined by the condition that all invariants $s_{lm} = 2P_l \cdot P_m$, constructed out of the four-momenta of any two neighboring partons/parton-heavy quark pairs l and m in the color-ordered subamplitudes [16], are larger than a cut-off value s_{min} . The soft and collinear region corresponds to the case where one or two of the s_{ij} are smaller than s_{min} . In the hard phase space region, one can work in four dimensions and perform the phase space

integration numerically. In the soft and collinear region, the integration is done analytically in d dimensions using soft and collinear approximations, which are valid in the limit that s_{\min} is small. The cross section in this region again factorizes into a universal factor multiplying the Born cross section. The initial state collinear singularities are factorized into parton distribution functions in the $\overline{\text{MS}}$ scheme, using the formalism of crossing functions [1].

Note that the process $ij \rightarrow W Q \bar{Q}$ is quite different from the other subprocesses: the heavy quark does not originate from the W vertex, and it is independent of s_{\min} , because it is free from singularities.

Adding the real and virtual corrections leads to the cancellation of all remaining singularities. We checked gauge invariance for both the virtual and real corrections. One is finally left with a two-to-two particle contribution (consisting of Born, soft-plus-collinear-plus-virtual, and crossing function contributions) and the two-to-three particle contribution in the hard region.

Before showing any numerical results, we first list here the default choices we made for parameters and cuts in producing the results of this paper. Any deviation from these choices will be indicated explicitly. For the case of charm (bottom) we assumed three (four) light flavors and no charm (bottom) quark distribution function. We used both at LO and NLO the CTEQ3M [17] set of parton distribution functions, and the two-loop expression for the running coupling constant with a four flavor, two-loop $\Lambda_{\text{QCD}} = 0.239$ GeV, the value supplied with the CTEQ3M set. We implemented continuity across heavy flavor thresholds [18] using the parametrization of Ref. [19]. We used the Snowmass convention [20] for the definition of a jet. Our conditions on the transverse energy and pseudorapidity of the jet were $E_T(\text{jet}) > 10$ GeV, $|\eta_{\text{jet}}| < 3$. We took a jet cone size of $\Delta R = 0.7$, and implemented no cuts on the W . We took the mass of the W -boson $m_W = 80.23$ GeV, the heavy quark mass m equal to 1.7 GeV for charm and 5 GeV for bottom. We used $V_{cs} = 0.97$ and $V_{cd} = 0.22$ for the relevant Cabibbo-Kobayashi-Maskawa matrix elements. We chose the factorization scale equal to the renormalization scale and denote it by μ , taking $\mu = m_W$. At least one heavy quark was required to be inside of the jet, with the sign of its electric charge correlated with the W charge, as in the LO diagram.

We first examine how the cross section changes when we vary the arbitrary parameters s_{\min} and μ . The dependence of the cross section and its two-to-two and two-to-three components on the choice of s_{\min} is shown in Fig. 2a for a wide s_{\min} range. It is clear from Fig. 2a that each of the two components depends strongly on the theoretical cut-off s_{\min} , but at low s_{\min} the cross section does not, see also Fig. 2b¹. At high s_{\min} the cross section varies because the soft and collinear approximations used are no longer reliable. We actually verified the s_{\min} independence in each order in the expansion in $1/N_c$, where $N_c = 3$ is the number of colors. The results shown in the remainder of this paper are averaged over s_{\min} between 1 and 10 GeV.

In Fig. 3 we show the renormalization/factorization scale dependence of the inclusive

¹Note that in this figure we used for $0.1 \text{ GeV} < s_{\min} < 10 \text{ GeV}$ larger statistics and smaller bins than for $s_{\min} > 10 \text{ GeV}$.

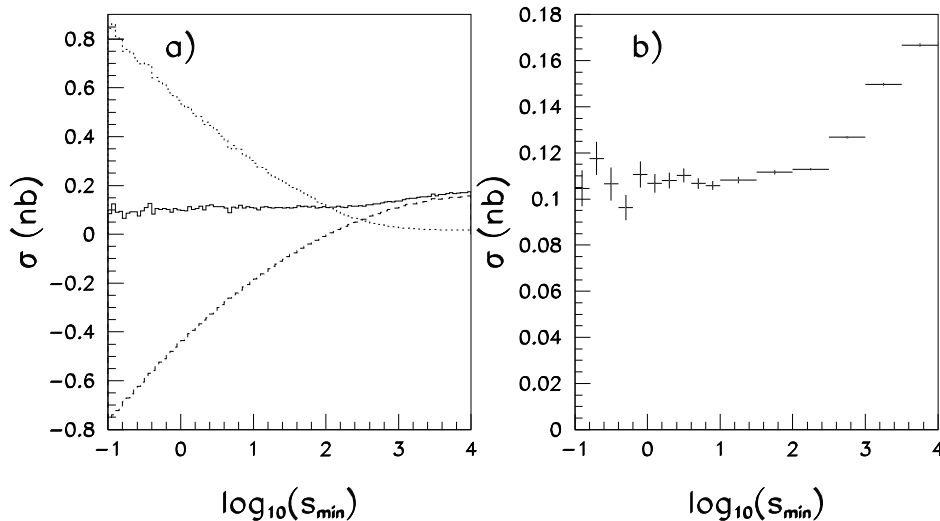


Figure 2: s_{\min} -dependence of $p\bar{p} \rightarrow W^+ +$ exclusive charm-tagged one-jet production. a) Solid histogram is for the total cross section, dashed histogram is for its two-to-two component, and the dotted one is for its two-to-three component. b) Total cross section; the error bars represent the statistical errors from the Monte-Carlo integration.

cross section, minus the $W + c\bar{c}$ contribution, along with the LO contribution. As expected, the inclusion of the NLO corrections reduces the scale sensitivity, albeit slightly. We show the $W + c\bar{c}$ contribution separately, because, as alluded to earlier, this contribution is technically of leading order. It therefore exhibits a strong scale dependence, as can be seen in Fig. 3.

3. The Strange Quark Distribution in the Proton

In this section we discuss the effect that the inclusion of the NLO QCD corrections to $W +$ charm-tagged jet production has on constraining the strange quark distribution function $s(x, \mu)$ in the proton. Here x is the momentum fraction of the strange quark in the proton, and μ is the factorization scale. For the sake of clarity we briefly summarize the study done in Ref. [7] using the shower Monte-Carlo program PYTHIA. At low scale μ , the strange quark distribution function can on the one hand be inferred from the appropriate linear combination of F_2 structure functions in neutrino and muon deep inelastic scattering [21]. On the other hand, it can also be determined from di-muon events in neutrino deep-inelastic scattering (DIS) [22]. Using current experimental data sets, the two methods yield a difference of about a factor of two for the strange quark distribution function at low μ . It was suggested in [7] that the strange quark distribution function can also be constrained by determining the charm content of $W + 1$ jet events at the Tevatron, since the leading order subprocess, $sg \rightarrow Wc$, is directly proportional to the strange quark distribution function. In this measurement the strange quark will effectively be probed at a larger scale $\mu \simeq M_W$.

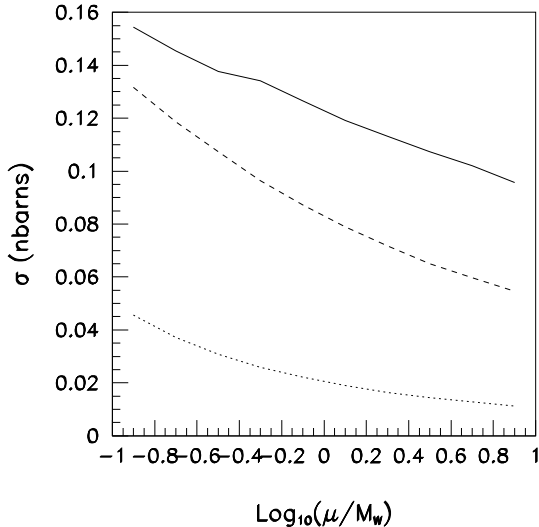


Figure 3: μ -dependence for $p\bar{p} \rightarrow W^+ +$ inclusive charm-tagged one-jet production. The solid line represents the NLO production (minus the $W + c\bar{c}$ contribution), the dashed line the LO production, and the dotted line the $W + c\bar{c}$ contribution.

set	mass (GeV)	LO	$WQ\bar{Q}$	NLO
CTEQ1M	$m_c=1.7$	96	20	161
MRSD0'	$m_c=1.7$	81	20	138
CTEQ3M	$m_c=1.7$	83	20	141
CTEQ3M	$m_b=5.0$	0.17	9.09	9.33

Table 1: The $W +$ charm-tagged one-jet inclusive cross section in pb for LO, $W + Q\bar{Q}$, and NLO (including the $W + Q\bar{Q}$ contribution) using different sets of parton distribution functions. The statistical uncertainty from the Monte-Carlo integration is less than 1%.

At this higher scale, the difference between the two strange quark distribution functions is smaller due to QCD evolution. When relevant backgrounds are included and standard cuts are used, the factor of two evolves into a difference of about 14% in the $W + c$ production cross section. The charm tagging efficiency required to distinguish the two cases at the one standard deviation level was found to be about 10% for 6000 $W + 1$ jet events.

In Table 1 we give the NLO cross section for the parton distribution function sets CTEQ1M and MRSD0'. The MRSD0' set derives its strange quark distribution from the di-muon data, whereas the CTEQ1M set uses the DIS data. Also shown is the result obtained with the more recent CTEQ3M set, which uses the same assumption about the strange quark distribution as MRSD0'. Comparing the CTEQ3M and MRSD0' sets, we see that the difference due to using more recent data sets in the global fit for the parton distribution functions is small. This is also reflected in the cross section for $W + c\bar{c}$, which

is the same for all three sets. We can conclude that the difference between CTEQ1M and MRSD0' of 15.4 % is due to the strange quark distribution function. This difference becomes 14.5% when one includes the $W + b$ background (9 pb, almost all of it coming from the gluon splitting contribution, see Table 1), and assuming conservatively that each bottom quark is mistagged as a charm quark. This shows that the conclusions reached in Ref. [7] are still valid at NLO. In both the NLO calculation and the PYTHIA analysis about 50% of the contributions are initiated by strange quarks. One major difference is that PYTHIA suggests that the gluon splitting contributes about 35%, whereas in the NLO calculation it is only about 15%. We found this number however to be quite sensitive to the choice of factorization and renormalization scale (recall we took M_W) in the gluon splitting contribution. Further phenomenological study of this question and others requires the inclusion of the W leptonic decay in our calculation.

4. The Mass Dependence of Jet Production

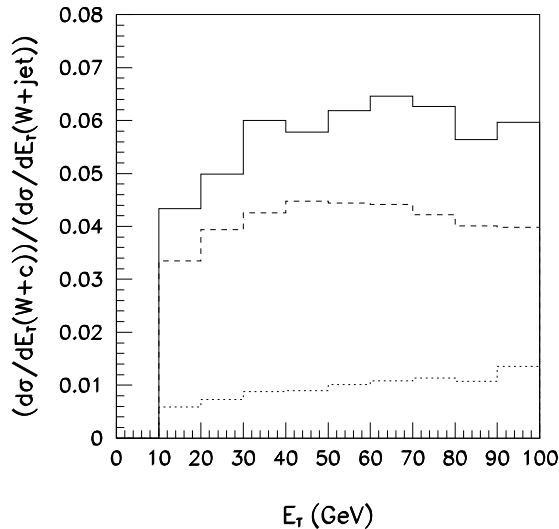


Figure 4: *Ratio of $W +$ charm-tagged inclusive one-jet production over $W +$ inclusive untagged one-jet production as function of the jet transverse energy. The solid line is the NLO ratio and the dashed line the LO ratio. The $W + c\bar{c}$ contribution to the NLO ratio is also shown (dotted line).*

A comparison can be made between $W +$ untagged jet production² [1] and $W +$ charm-tagged jet production. The most obvious quantity to study in this regard is the jet transverse energy ($E_T(\text{jet})$) distribution. In Fig. 4 we present the ratio of the charm-tagged jet over the untagged jet $E_T(\text{jet})$ -distribution for the LO and NLO cases. At LO the charm-tagged jet is simply represented by a charm quark. The ratio in Fig. 4 has a characteristic shape which can readily be understood at tree level. At low $E_T(\text{jet})$ the charm-tagged jet rate is

²For the untagged process we take five massless quark flavors.

suppressed relative to the untagged-jet rate due to its fermionic final state. The untagged-jet rate is dominated by the gluonic final state which has a soft singularity, that is absent for the fermionic final state. At high $E_T(\text{jet})$ we again observe a relative suppression of the charm-tagged jet because at LO this process has a gluon in the initial state. At high $E_T(\text{jet})$ the dominant scattering in the untagged-jet rate is due to quark-antiquark collisions, again favoring the gluonic final state. Apart from an approximate overall K -factor, the NLO cross section retains these features although the identification with the LO parton model is lost. Also shown in Fig. 4 is the $W + c\bar{c}$ contribution. At low $E_T(\text{jet})$ its suppression is more pronounced due to the charm quark pair production threshold. At high $E_T(\text{jet})$ there is no suppression for this process because it is instigated by a quark-antiquark collision.

Thus we see that the $E_T(\text{jet})$ behaviour of tagged jets is basically as expected. We now turn to the mass dependence of the cross section. In the LO calculation, one may take the charm mass to zero, and, within Monte-Carlo errors, obtain a result which is identical to the massive case. However, we will now show that there are important mass effects at NLO, especially when we look in detail at the tagged jets. In fact, taking the heavy quark mass to zero in the NLO calculation leads to a divergence.

Let us first consider the $W + Q\bar{Q}$ contribution. Because the mass of the heavy quark regulates the collinear singularity, it is expected that the strongest mass dependence will come from the collinear region. In this region the cross section factorizes into the cross section for $W + \text{gluon}$ production multiplied by a universal factor. After integration over the invariant mass of the heavy quark pair we find that the mass dependent part of this universal factor has the following form:

$$\alpha_s \frac{N_c}{8\pi} P_{q\bar{q}\rightarrow g}(z) \ln\left(\frac{M^2}{m^2}\right) dz \quad (1)$$

where M is the upper limit of the heavy quark pair invariant mass defining the collinear region, and $P_{q\bar{q}\rightarrow g}(z)$ is the massless Altarelli-Parisi [23] splitting function:

$$P_{q\bar{q}\rightarrow g}(z) = \frac{2}{N_c}(z^2 + (1-z)^2). \quad (2)$$

There is some ambiguity in the definition of z . Here, we choose the following:

$$z = \frac{E + P_{\parallel}}{E_{jet} + P_{jet}} \quad (3)$$

where E and P_{\parallel} are the heavy quark energy and momentum projected on the jet direction, and E_{jet} and P_{jet} are the jet energy and momentum. We have checked that other choices, such as $z = E_T(Q)/E_T(\text{jet})$, do not change any of the conclusions in what follows. In the strictly collinear limit M is much smaller than the energy of the gluon, but in a leading logarithmic approximation one may take M to be of the order of $E_T(\text{jet})$. The behavior of Eq. (1) can be seen qualitatively in Fig. 5a, where the ratio of the $W + c\bar{c}$ cross section over the $W + \text{gluon}$ cross section is shown as a function of the transverse energy of the jet. One can see an approximate logarithmic enhancement with increasing E_T , as predicted by the leading logarithmic approximation. On the other hand, the z -distribution, plotted in

Fig. 5b, does not conform with the z -dependence described by Eq. (1). First, the peak at $z = 1$ is due to events where the \bar{Q} is not inside of the jet, such that the whole jet is formed by the lone Q . Second, the cross section is suppressed near $z = 0$ and $z = 1$ (excluding the peak) due to terms in the collinear region that depend strongly on z , but not on M . One

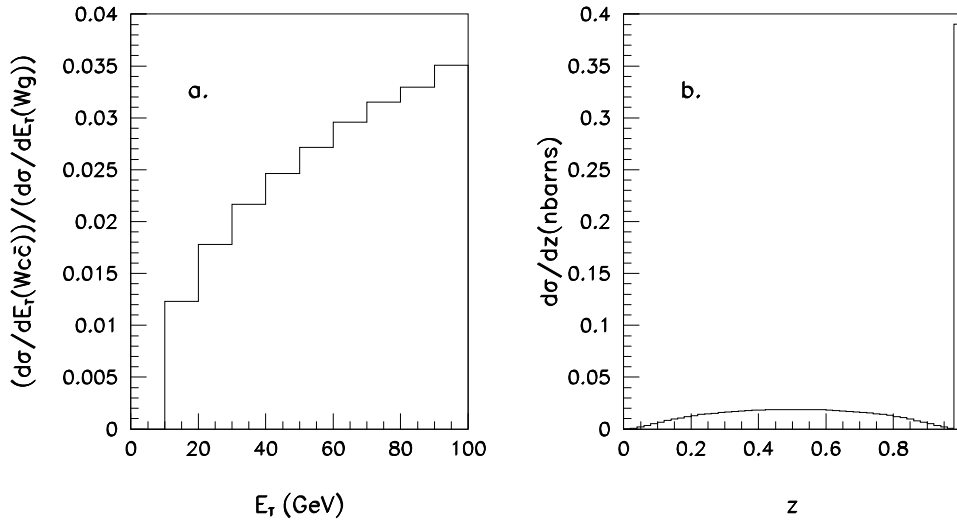


Figure 5: *a) Ratio of the $W + c\bar{c}$ component of the charm-tagged one-jet inclusive cross section to the $W +$ gluon cross section, as a function of the jet transverse energy. b) The z -distribution of the $W + c\bar{c}$ component.*

way to enhance the effect of the leading logarithm term of Eq. (1) in the z distribution is to lower the mass of the heavy quark in our calculation. This is done in Fig. 6a, where we show the z -distribution for the case $m = 0.01$ GeV. Clearly it now resembles the functional form of Eq. (2) much closer.

The $\ln(m^2)$ term in Eq. (1) diverges in the limit of vanishing quark mass, and is not cancelled by any other contribution³. In principle, any observable should be “collinear safe”, i.e. if the mass is taken to zero, the observable should be finite and approach the massless result. This is needed to describe situations where the relevant scale is much larger than the heavy quark mass. In the present case we are dealing with a final state divergence in $\ln(m^2)$ that should be factorized into the fragmentation function of the gluon into a heavy hadron. It is only after the proper introduction of the fragmentation function in the calculation that the massless limit will be finite. The evolution of fragmentation functions will resum the large logarithms $\ln(E_T^2)$. This problem is the final state version of the problem of heavy quark distribution functions [24]. It is beyond the scope of this short letter, but we will discuss it in more detail in [9]. Some studies in this regard were done in Ref. [25]. Here, we simply keep the mass finite.

³In the $W + 1$ jet calculation, this singularity is cancelled by a companion collinear singularity in the quark-loop correction to the outgoing gluon in the Born diagram. In our calculation this diagram is not present.

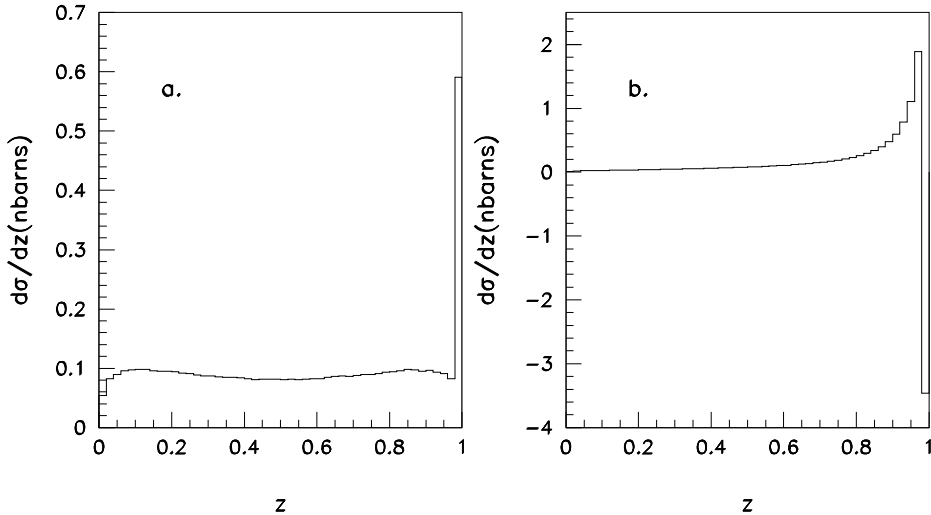


Figure 6: *The z -distribution of the charm-tagged one-jet inclusive cross section, with $m = 0.01$ GeV. a) $Wc\bar{c}$ component. b) Total contribution minus the $Wc\bar{c}$ component.*

Let us now turn to the NLO single charm contribution (excluding the $W + c\bar{c}$ contribution). In the collinear region, the cross section again factorizes, leading, after integration over the invariant mass of the collinear partons, to the universal factor:

$$\alpha_s \frac{N_c}{8\pi} P_{qg \rightarrow q}(z) \ln \left(\frac{M^2}{m^2} \right) dz \quad (4)$$

where $P_{qg \rightarrow q}(z)$ is the splitting function:

$$P_{qg \rightarrow q}(z) = \lim_{\delta \rightarrow 0} 2 \left(1 - \frac{1}{N_c^2} \right) \left(\left(\frac{1+z^2}{1-z} \right) \theta(1-z-\delta) + \left(\frac{3}{2} + 2 \ln \delta \right) \delta(1-z) \right). \quad (5)$$

In Fig. 6b we show for the single charm quark contribution the z -distribution, with the contribution of Eq. (4) enhanced by taking $m = 0.01$ GeV. Note that it resembles the functional form in Eq. (5). From Eq. (5) one derives

$$\int_0^1 P_{qg \rightarrow q}(z) dz = 0, \quad (6)$$

which must hold for the probability to find a quark in a quark of the same flavor to be one [23]. From Eqs. (6) and (4) we can now make the important observation that as long as the cuts on the heavy quark-tagged jet are such that all z -values are allowed to contribute, there are no large logarithms $\ln(E_T^2/m^2)$. However, if the cuts are such that the z -integration is restricted, or convoluted with a z -dependent function, some $\ln(E_T^2/m^2)$ terms will remain. An example of such a convolution is the E_T distribution of the heavy quark itself. All this is illustrated in Fig. 7a, where two cases of z -restrictions ($z > 0.9$ and $z < 0.9$) are plotted in addition to the all- z case. Note that for the all- z case the ratio is indeed essentially independent of $E_T(\text{jet})$, but that for the z -restricted cases the logarithmic dependence is

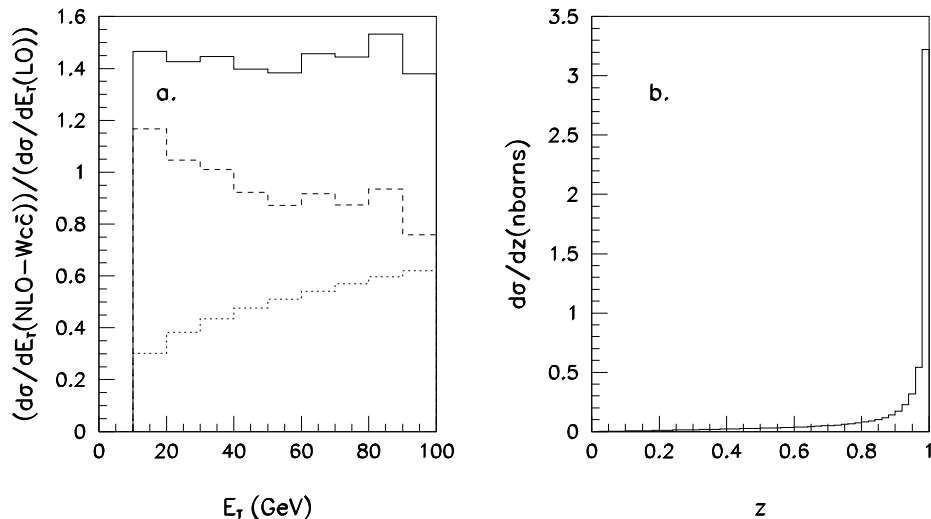


Figure 7: a) E_T distribution ratio of NLO charm-tagged one-jet inclusive cross section to LO one. Solid line has no restrictions on the z -integration, the dotted and dashed line have restrictions of $z < 0.9$ and $z > 0.9$ respectively. b) z -distribution of NLO charm-tagged one-jet inclusive cross section. The $W + c\bar{c}$ component is not included in these plots.

apparent. For completeness we show in Fig. 7b the z -distribution for the single charm contribution for $m = 1.7$ GeV.

Thus care must be taken when calculating tagged cross sections in determining whether or not there are large logarithms present due to restrictions on the z -integration. Such restrictions would also necessitate the introduction of the appropriate fragmentation function to absorb the $\ln(m^2)$ terms, as in the $WQ\bar{Q}$ case.

Note that for the example of the jet transverse energy distribution given in Fig. 4 there is no constraint on the z -integration, so that the only logarithmic mass term is due to the $Wc\bar{c}$ contribution.

5. Conclusions

We have completed the first calculation of the QCD corrections to $O(\alpha_s^2)$ of the reaction $p\bar{p} \rightarrow W + Q$. In this short paper we briefly summarized the method of calculation. We demonstrated that the inclusion of the NLO corrections does not change the conclusions of Ref. [7] about constraining the strange quark distribution function using $W +$ charm-tagged jet events at the Tevatron. However, since we now have a NLO calculation, this procedure will be able to constrain the NLO strange quark distribution, once a reasonable data sample is collected. Finally we studied the E_T distribution of the jet containing the heavy quark and the mass dependence of the cross section. We noted the need to include the leptonic decay of the W and the heavy hadron fragmentation functions in our calculation, in order to be able to do more extensive phenomenological studies.

References

- [1] W.T. Giele, E.W.N. Glover, and D.A. Kosower, Nucl. Phys. **B403** (1993) 633.
- [2] S. Abachi et al (D0 collaboration), Phys. Rev. Lett. **75** (1995) 3226.
- [3] R. Blair for the CDF collaboration, FERMILAB-CONF-95/245-E. Presented at 10th Topical Workshop on Proton-Antiproton Collider Physics, Batavia, IL, 9-13 May 1995.
- [4] F. Abe et al (CDF Collaboration), Nucl. Instrum. Meth. **A289** (1990) 388; Nucl. Phys. **B27** (1992) 246 (Proc. Suppl).
- [5] F. Abe et al (CDF collaboration), Phys. Rev. Lett. **74** (1995) 2626; S. Abachi et al (D0 collaboration), Phys. Rev. Lett. **74** (1995) 2632.
- [6] W.T. Giele. and E.W.N. Glover, FERMILAB-CONF-95-168-T. Presented at 10th Topical Workshop on Proton-Antiproton Collider Physics, Batavia, IL, May 1995.
- [7] U. Baur, F. Halzen, S. Keller, M.L. Mangano and K. Riesselmann, Phys. Lett. **B318** (1993) 544.
- [8] H.-U. Bengtsson and T. Sjöstrand, Comp. Phys. Comm. **46** (1987) 43; T. Sjöstrand, preprint CERN-TH.6488/92.
- [9] W.T. Giele, S. Keller and E. Laenen, in preparation.
- [10] W.T. Giele and E.W.N. Glover, Phys. Rev. **D46** (1992) 1980. For equivalent methods see H. Baer, J. Ohnemus, and J. F. Owens, Phys. Rev. **D40** (1989) 2844; S. Frixione, M.L. Mangano, P. Nason and G. Ridolfi, Nucl. Phys. **B403** (1993) 633.
- [11] W. Beenakker, Ph.D. thesis, unpublished.
- [12] G. Passarino and M. Veltman, Nucl. Phys. **B160** (1979) 151.
- [13] FORM2 by J.A.M. Vermaseren, Published by Computer Algebra Netherlands (CAN), Kruislaan 413, 1098 SJ Amsterdam, The Netherlands.
- [14] J.C. Collins, F. Wilczek, and A. Zee, Phys. Rev. **D18** (1978) 242;
- [15] M.L. Mangano, Nucl. Phys. **B403** (1993) 536.
- [16] F.A. Berends and W.T. Giele, Nucl. Phys. **B306** (1988) 759; M.L. Mangano, Nucl. Phys. **B309** (1988) 461.
- [17] H.L. Lai et al, Phys. Rev. **D51** (1995) 4763.
- [18] J.C. Collins and W-K. Tung Nucl. Phys. **B278** (1986) 934.
- [19] G. Altarelli, M. Diemoz, G. Martinelli and P. Nason, Nucl. Phys. **B308** (1988) 724.
- [20] J.E. Huth et al, in proceedings of the Snowmass Workshop, *High Energy Physics in the 1990's*, Snowmass, Colorado, July 1990, p. 134.

- [21] J. Botts et al, Phys. Lett. **304B** (1993) 159.
- [22] W.H. Smith et al (CCFR Collaboration), in proceedings of ICHEP 92, Dallas, 1992, J.R. Sanford, ed.
- [23] G. Altarelli and G. Parisi, Nucl. Phys. **B126** (1977) 298.
- [24] M.A.G. Aivazis, J.C. Collins, F.I. Olness and W-K. Tung, Phys. Rev. **D50** (1994) 3102.
- [25] M. Cacciari and M. Greco, Nucl. Phys. **B421** (1994) 530; B. Kniehl, M. Krämer, G. Kramer and M. Spira, Phys. Lett. **356B** (1995) 539; M. Cacciari and M. Greco preprint DESY 95-103.